

AD-A242 378



AD-A242 378

MARCH 1980

AD-A242 378



EXPERIMENTS ON LOW ASPECT RATIO HYDROPLANES TO MEASURE LIFT UNDER STATIC AND DYNAMIC CONDITIONS

DISTRIBUTION STATEMENT A

Approved for public release
Distribution Unlimited

B Ward

A R J M Lloyd

Original contains color
plates. All DTIC representa-
tions will be in black and
white.

91-15451



This document is the property of Her Majesty's Government
and Crown copyright is reserved. Requests for permission
to publish its contents outside official circles should be
addressed to the Issuing Authority.

Best Available Copy

ADMIRALTY RESEARCH ESTABLISHMENT
Procurement Executive Ministry of Defence
Hosier GOSPORT Hants PO12 2AG

UNLIMITED

DTIC
ELECTE
NOV 12 1991
S B D

0072650

CONDITIONS OF RELEASE

BR-114028

DRIC U

COPYRIGHT (c)
1988
CONTROLLER
HMSO LONDON

DRIC Y

Reports quoted are not necessarily available to members of the public or to commercial organisations.

ARE TM(UHR)90306

MARCH 1990

EXPERIMENTS ON LOW ASPECT RATIO HYDROPLANES
TO MEASURE LIFT UNDER STATIC AND DYNAMIC CONDITIONS

By

B Ward
A R J M Lloyd

Summary

This Technical Memorandum describes experiments in the Circulating Water Channel to measure lift forces on low aspect ratio hydroplanes under static and dynamic conditions. Empirical equations to represent the results are given.

Admiralty Research Establishment
Haslar GOSPORT Hants PO12 2AG

C
Copyright
Controller HMSO London
1990

Contents

	Page
Notation	iv
1. Introduction	1
2. The Experiment	1
3. Data Acquisition and Data Analysis	1
4. Static Runs	2
5. Oscillating Runs	2
6. Ramping Motions	2
7. Empirical Equations	3
8. Effects due to Thickness Ratio	5
9. Effects due to Faired Tips	5
10. Random Signal Experiments	6
11. Conclusions	6
References	7
Figure 1. Three NACA 0020 Hydroplanes	
Figure 2. Hydroplane on Servo	
Figures 3 and 4. Experiment in Circulating Water Channel	
Figure 5. Resolution of Forces on the Hydroplane	
Figure 6. Static Time History	
Figure 7. Lift Coefficient - Aspect Ratio 1, Static Condition	
Figure 8. Lift Coefficient - Aspect Ratio 1.5, Static Condition	
Figure 9. Lift Coefficient - Aspect Ratio 2, Static Condition	
Figure 10. Stall Angle - Static Condition	
Figure 11. Dynamic Time History	
Figure 12. Lift Coefficient - Aspect Ratio 1, Dynamic Condition	
Figure 13. Lift Coefficient - Aspect Ratio 1.5, Dynamic Condition	
Figure 14. Lift Coefficient - Aspect Ratio 2, Dynamic Condition	

- Figure 15. Phase Angle - Aspect Ratio 1
- Figure 16. Phase Angle - Aspect Ratio 1.5
- Figure 17. Phase Angle - Aspect Ratio 2
- Figure 18(i). Dynamic Condition - Aspect Ratio 2, 35.5 Degrees
Frequency 0.055Hz, $\frac{\omega C}{U} = 0.036$
- Figure 18(ii). Dynamic Condition - Aspect Ratio 2, 35.5 Degrees
Frequency 0.168Hz, $\frac{\omega C}{U} = 0.11$
- Figure 18(iii). Dynamic Condition - Aspect Ratio 2, 35.5 Degrees
Frequency 0.222Hz, $\frac{\omega C}{U} = 0.145$
- Figure 19. Example of Delayed Stall - Aspect Ratio 1.5, 41 Degrees
Angular Rate 6 degrees/sec
- Figure 20. Empirical Formula for Coefficient a_0 Representing Lift
Curve Slope
- Figure 21. Empirical Formula for Coefficient a_1
- Figure 22. Empirical Formula for Coefficient a_2
- Figure 23. Effect of Thickness on Lift Curve Slope
NACA 00xx Series, Aspect Ratio 6, $Re = 4 \times 10^6$
- Figure 24. Comparison of Empirical Formula with Random Signal
Results



Accession For	
NTIS GRA&I	<input checked="" type="checkbox"/>
DTIC TAB	<input type="checkbox"/>
Unannounced	<input type="checkbox"/>
Justification	
By	
Distribution/	
Availability Codes	
Dist	Avail and/or Special
A-1	

Notation

A	Surface Area of Hydroplane	m ²
a ₀	Coefficient of Empirical Equation 3 - Lift Curve Slope for t/c = 0.2	rad ⁻¹
a' ₀	Modified Coefficient of Empirical Formula 3 for given t/c	
a ₁	Coefficient of Empirical Equation 3	
a ₂	Coefficient of Empirical Equation 3	
a _e	Aspect Ratio of Hydroplane 2s/c	
c	Chord length	m
C _L	Lift Coefficient	
C _{L0}	Lift Coefficient Amplitude	
D	Drag Force: Positive to Tail	N
L	Lift Force: Positive Nose to Port	N
N	Force Normal to Hydroplane Positive to Port	N
Re	Reynolds Number	
U	Flow Velocity	m/s
s	Span	m
T	Force Tangential to Hydroplane Positive Forward	N
t	Thickness at quarter chord of hydroplane	m
α	Angle of Incidence Positive Nose to Port	degrees
α _{ST}	Stall Angle of Incidence for t/c = 0.2	radians
α' _{ST}	Stall Angle of Incidence for given t/c	radians
α̇	Angular velocity	radians/sec
α̈	Angular Acceleration	radians/sec
ε	Phase Angle	radians
ρ	Density of Fresh Water	1000 tonnes/m ³

ω	Frequency	radians/sec
Ω	Sweep Angle	radians

EXPERIMENTS ON LOW ASPECT RATIO HYDROPLANES TO MEASURE LIFT UNDER STATIC AND DYNAMIC CONDITIONS

By B Ward and A R J M Lloyd

1. INTRODUCTION

In support of SUBSIM (Reference 1) the computer program which simulates submarine manoeuvres, there was a need for data on dynamic effects on lift forces for low aspect ratio hydroplanes. A thorough literature search was carried out; previous papers usually described two dimensional experiments at much higher frequencies than those of relevant interest. It was therefore decided to perform some dedicated experiments to obtain the required data.

2. EXPERIMENT

Three NACA 0020 hydroplanes were used of aspect ratios 1, 1.5 and 2 (Figure 1). Each hydroplane had a chord length of 0.26 m and span of 0.13 m, 0.195 m and 0.26 m respectively. A strain gauged stock at the quarter chord position of the hydroplane was attached to a servo to oscillate the hydroplane (Figure 2). The same stock was used for all three hydroplanes. Strain gauge bridges on the stock were calibrated to give normal and tangential forces.

The experiment was conducted in the Circulating Water Channel (Figures 3 and 4). The servo was attached below the CWC floor and the position of the floor was altered to accommodate each hydroplane. A 1 mm space was left between the floor and the hydroplane root. Horizontal flow velocity was maintained at 2.5 m/s.

3. DATA ACQUISITION AND DATA ANALYSIS

The DATS computer package was used for both data acquisition and data analysis. DATS consists of a number of modules which enable mathematical functions to be applied to files of time history data (see DATS User Manual, Reference 2).

Velocity of the flow was measured upstream of the hydroplane using laser doppler velocimetry techniques.

Velocities from the laser, achieved angle from the servo, and normal and tangential forces from the stock were acquired simultaneously. The lift was derived from (see Figure 5)

$$L = N \cos \alpha + T \sin \alpha \quad (1)$$

The upper tangential force gauge was damaged when the experiment was being rigged and no measurements of total tangential force were possible. The readings from the lower gauge were doubled to allow equation (1) to be used to calculate the lift force. This procedure was not strictly correct but will not have introduced any large errors because the contribution of the tangential force to the lift is very small.

Lift coefficients were calculated using the instantaneous velocity.

$$C_L = \frac{L}{\frac{1}{2}\rho U^2 A} \quad (2)$$

4. STATIC RUNS

Mean values of α and C_L were taken for static runs over the acquisition time; typically 50 seconds (Figure 6).

Figures 7 to 9 show plots of non dimensional lift C_L against angle of attack for aspect ratios 1, 1.5 and 2 respectively.

Figure 10 shows a plot of stall angle against aspect ratio.

5. OSCILLATING RUNS

Oscillating runs (Figure 11) were carried out at frequencies from 0.055 Hz to 0.386 Hz corresponding to $\frac{\omega c}{U}$ values from 0.036 to 0.252.

Frequencies were chosen to correspond to full scale angular rates in the region of 5 degs/sec. The frequency was limited to ensure that rate limiting did not occur in the servo. The average C_L amplitudes were calculated. Plots are shown in Figures 12 to 14. Little variation with frequency was apparent.

Figures 15 to 17 show plots of phase angles against $\frac{\omega c}{U}$ for three different aspect ratios. The phase angles are positive indicating that lift leads incidence. Note the linear trend in the data.

Figure 18(i) to 18(iii) shows continuous plots of C_L against incidence for three oscillating runs with aspect ratio 2 at different frequencies. Incidence amplitude is 35.5 degrees in all cases (above the static stall angle). Note at the lower frequency stall is evident. At the higher frequencies the lift coefficient is higher at zero angle corresponding to greater phase lead. Stalling does not seem to occur at the high frequencies.

6. RAMPING MOTIONS

Figure 19 shows the results of three ramping motion experiments to an incidence of 41 degrees at 6 degs/sec ($\frac{\dot{\alpha} c}{U} = 0.011$) for an aspect ratio of 1.5. In each case the lift coefficient follows the angle of incidence to well above the maximum static value. In other words the hydroplane does not immediately stall. After some time flow separation occurs, the hydroplane stalls and the lift collapses to the value given in Figure 8. High lift is maintained for an apparently arbitrary time.

7. EMPIRICAL EQUATIONS

7.1. Representation of C_L by Second-Order Linear Equations

It is assumed that under dynamic conditions the equation for lift coefficient is

$$C_L = a_0 \alpha + a_1 \dot{\alpha} \frac{c}{U} + a_2 \ddot{\alpha} \frac{c^2}{U^2} \quad (3)$$

where $a_0 \alpha$ is the static lift curve slope, $a_1 \dot{\alpha}$ is the effect of angular rate and $a_2 \ddot{\alpha}$ is the acceleration effect.

The following equations can then be derived

$$\alpha_0 \left(-a_2 \frac{c}{U^2} \omega^2 \cos \epsilon - a_1 \frac{c}{U} \omega \sin \epsilon + a_0 \cos \epsilon \right) = C_{L0} \quad (4)$$

where α_0 is the α amplitude

and C_{L0} is the C_L amplitude

and

$$\epsilon = \tan^{-1} \left[\frac{-\frac{c}{U} a_1 \omega}{a_0 - a_2 \omega^2 \frac{c^2}{U^2}} \right] \quad (5)$$

Using the experiment results and the least squares plane method the coefficients in equation (4) were derived for each of the three aspect ratios;

a_e	a_2	a_1	a_0
1	0.37	1.12	1.72
1.5	0.44	1.3	1.95
2	0.47	1.4	2.12

The experiment gave lower values than the empirical equation (6) derived by Whicker and Fehlner (Reference 3) at aspect ratio 1.5 and 2:

$$a_0 = \frac{1.8 \pi a_e}{1.8 + \sqrt{4 + a_e^2}} \text{ per radian} \quad (6)$$

That particular experiment used a NACA 0015 section as opposed to the NACA 0020 used in this study. NACA 0020 sections give reduced values of C_L compared with NACA 0015 (Reference 4). However at aspect ratio 1 the Whicker and Fehlner equation gives lower values than this experiment justifying the conclusion made in Reference 5 - 'that the lift curve slope at very low aspect ratios is seriously under estimated by equation (6)'. Although that conclusion was based on only two results, the results from this experiment give added weight to the statement. Using these assumptions and taking the lift curve slope to be zero at zero aspect ratio formed the basis under which a more general equation was derived for coefficient a_0 ie the lift curve slope:

$$\begin{aligned} a_0 &= 163 \tanh (0.5 a_e + 2.4) - 160 && \text{per radian } a_e \leq 2 \\ &= \frac{1.66 a_e}{1.8 + \cos \Omega \sqrt{4 + a_e^2 / \cos^4 \Omega}} && \text{per radian } a_e > 2 \end{aligned} \quad (7)$$

A plot can be seen in Figure 20.

As can be seen from Figures 7 to 9 the equation fits the linear part of the experiment data for static conditions very well.

Equations were derived to fit the coefficients a_1 and a_2 in equation (3).

Only three points are available and it was assumed that there are no dynamic effects if aspect ratio is zero. It was assumed that the function approaches limits determined by the trend of the data available. A plot of the equations for coefficients a_1 and a_2 can be seen in Figures 21 and 22 respectively.

$$a_1 = 99.3 \tanh (0.61 a_e + 2.42) - 97.7 \quad (8)$$

$$a_2 = 1.21 \tanh (0.78 a_e + 0.68) - 0.71 \quad (9)$$

The satisfactory fit of the equations can be seen in Figures 12 to 17.

Equation (5) for phase, compared with experimental results in Figures 15 to 17, is best for $a_e = 2$ and adequate for the lower aspect ratios.

7.2. Equation for Stall Angle

An empirical equation was derived from the experiment data on stall angle

$$\alpha_{ST} = 0.113 a_e^2 - 0.615 a_e + 1.32 \text{ radians} \quad (10)$$

This gives higher values for all three aspect ratios than that calculated by the formula used in SUBSIM (Reference 1)

$$\alpha_{ST} = 0.075 a_e^2 - 0.445 a_e + 1.05 \text{ radians} \quad (11)$$

which is derived from the data in Reference 3. These equations are compared with the experiment data in Figure 10.

The above equation is valid for $1 < a_e < 2$.

8. EFFECTS DUE TO THICKNESS CHORD RATIO

8.1. Correction for Lift Curve Slope

From results quoted in Reference 4, (Figure 23) it can be seen that a change in thickness ratio has an effect on lift curve slope. From these data the following formula has been derived to correct for thickness/chord ratio.

$$a'_0 = (0.96 + 1.7 t/c - 7.1 t^2/c^2) a_0 \quad (12)$$

The formula is valid for data in the range $t/c = 0.09$ to 0.35 .

8.2. Correction for Stalling Angle

Reference 3 gives stall angle data for square tip fins. Using those results and the results from this experiment a general equation for stall angle was derived correcting for thickness ratio.

$$\alpha'_{ST} = (0.36 + 3.2 t/c) \alpha_{ST} \quad (13)$$

9. EFFECTS DUE TO FAIRED TIPS

An unpublished report by the Stevens Institute of Technology discusses the fact that square tip hydroplanes give greater lift forces than faired tip hydroplanes. This was also noted in Reference 3 by Whicker and Fehlner. The conclusion reached in the Stevens report was that the hydroplane tip outboard of the trailing edge span can be assumed to carry no lift. This should be taken into account in SUBSIM by specifying the hydroplane outreach to exclude any faired tip.

10. RANDOM SIGNAL EXPERIMENTS

Following the experiments described in this report a further experiment (Reference 6) was conducted. The 1.5 aspect ratio hydroplane was oscillated using a random signal. Figure 24 shows a plot comparing the lift coefficient derived from equation (3) and a time history of C_L from the random signal experiment. The comparison is very good, confirming the validity of equation (3).

11. CONCLUSIONS

The experiment to examine dynamic effects on oscillating hydroplanes showed the effects to be small but worth noting. The most interesting aspect of the experiment was the delayed stall noted during the ramping motion experiments.

The rapid change in flow velocity at the surface of the hydroplane as it is ramped over causes a rapid change in pressure gradient. There is a delay in the build up of the adverse pressure gradient which allows the hydroplane to support greater lift than during the steady state. This was noted by Ericsson in Reference 7. According to Moore (Reference 8) this delay allows the hydroplane to respond to the change of angle of attack without stall which contributes to the lift overshoot.

Above the stall angle oscillating motions show increased values for C_L compared with static results due to dynamic effects.

No significant variation in C_L was noted over the range of frequencies examined. Phase angles are small; a phase lead of approximately 10 degrees occurs at the highest frequency of 0.386Hz ($\frac{\omega C}{U} = 0.252$). This may be significant for autopilot design.

Effects due to thickness ratio and faired tips should be considered when incorporating any empirical formula derived from this experiment into SUBSIM.

Empirical formulae fit experimental results very well. These formulae should be incorporated into the SUBSIM mathematical model and assessed by further validation of submarine predictions against full scale trial results.

REFERENCES

1. A R J M Lloyd. A Theory for Submarine Manoeuvring SUBSIM (Issue 3) (U). ARE TR89301. January 1989. UNCLASSIFIED.
2. DATS User Manual. PROSIG Computer Consultants Limited.
3. L F Whicker, L F Fehlner. Free Stream Characteristics of a Family of Low Aspect Ratio all Moveable Control Surfaces for Application to Ship Design. DTMB Report 933. December 1958. UNCLASSIFIED.
4. W K Bullivant. Tests of the NACA 0025 and 0035 Airfoils in the Full-Scale Wind Tunnel. NACA Report 708, 1941. UNCLASSIFIED.
5. A R J M Lloyd. Roll Stabiliser Fins: A Design Procedure. TRINA. Vol 117, 1975, p 233.
6. M Smith. Lift Coefficient of a Randomly Oscillating Hydroplane. To be published.
7. L E Ericsson. Comment on Unsteady Airfoil Stall. Journal of Aircraft Vol 4, No 5, September-October 1967.
8. F K Moore. Lift Hysteresis - Boundary Layer. NACA TN 1291. UNCLASSIFIED.
9. S F Hoerner, H V Borst. Fluid Dynamic Lift. Published by Mrs L A Hoerner, Hoerner Fluid Dynamics, PO Box 342, Brick Town TJ 08723. 1975.



FIG.1 THREE NACA 0020 HYDROPLANES

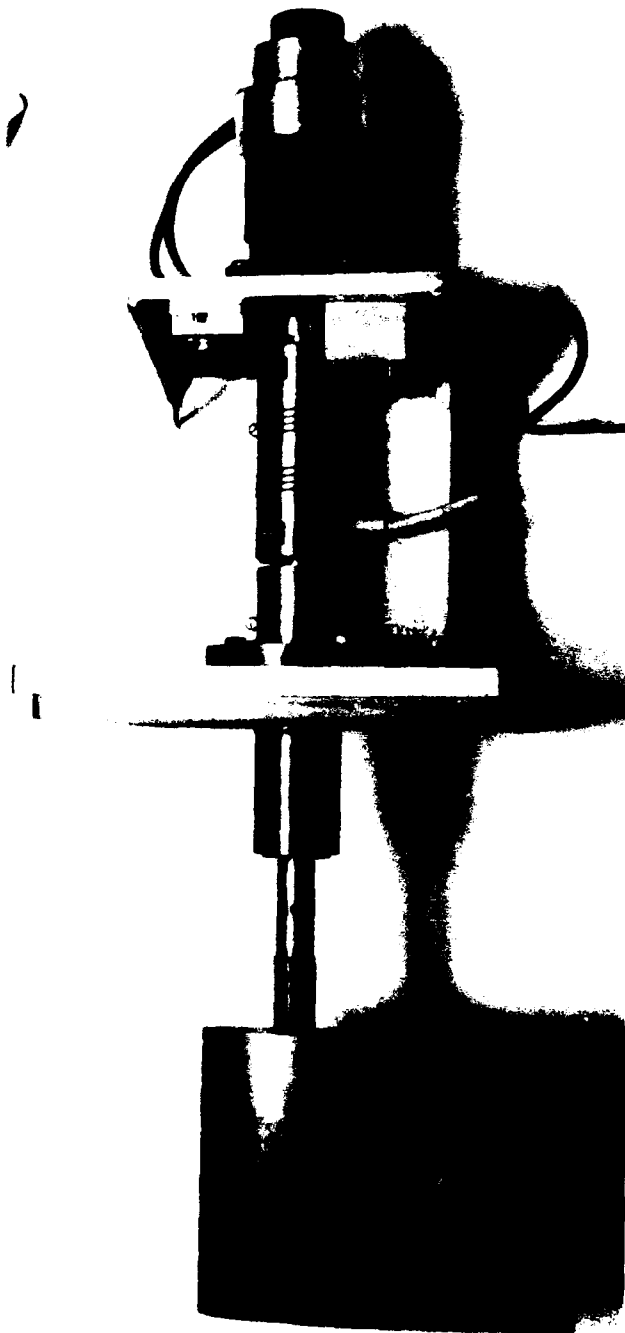


FIG.2 HYDROPLANE ON SERVO



FIG.3 EXPERIMENT IN CIRCULATING WATER CHANNEL



FIG.4 EXPERIMENT IN CIRCULATING WATER CHANNEL

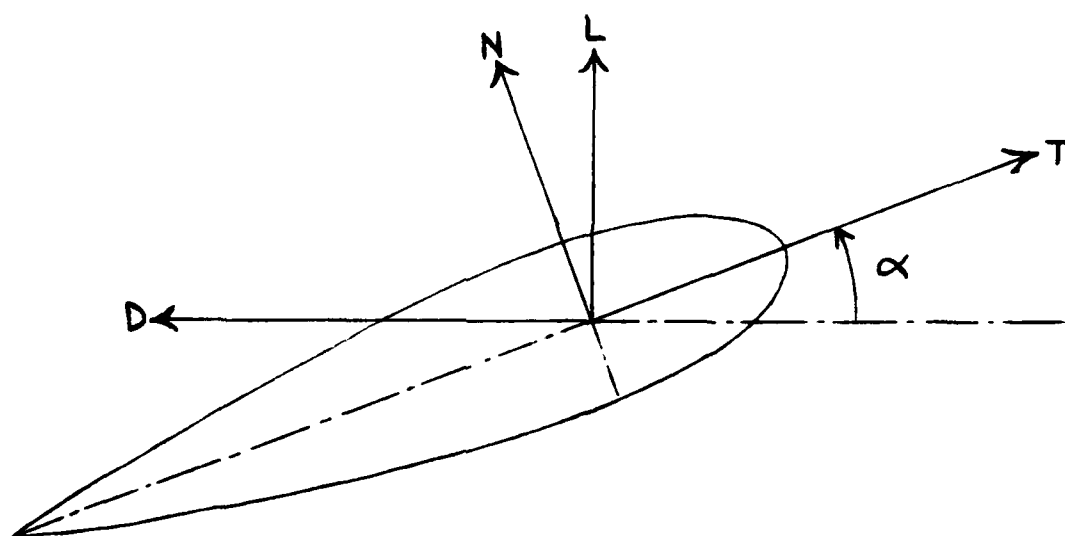


FIG.5 RESOLUTION OF FORCES ON HYDROPLANE

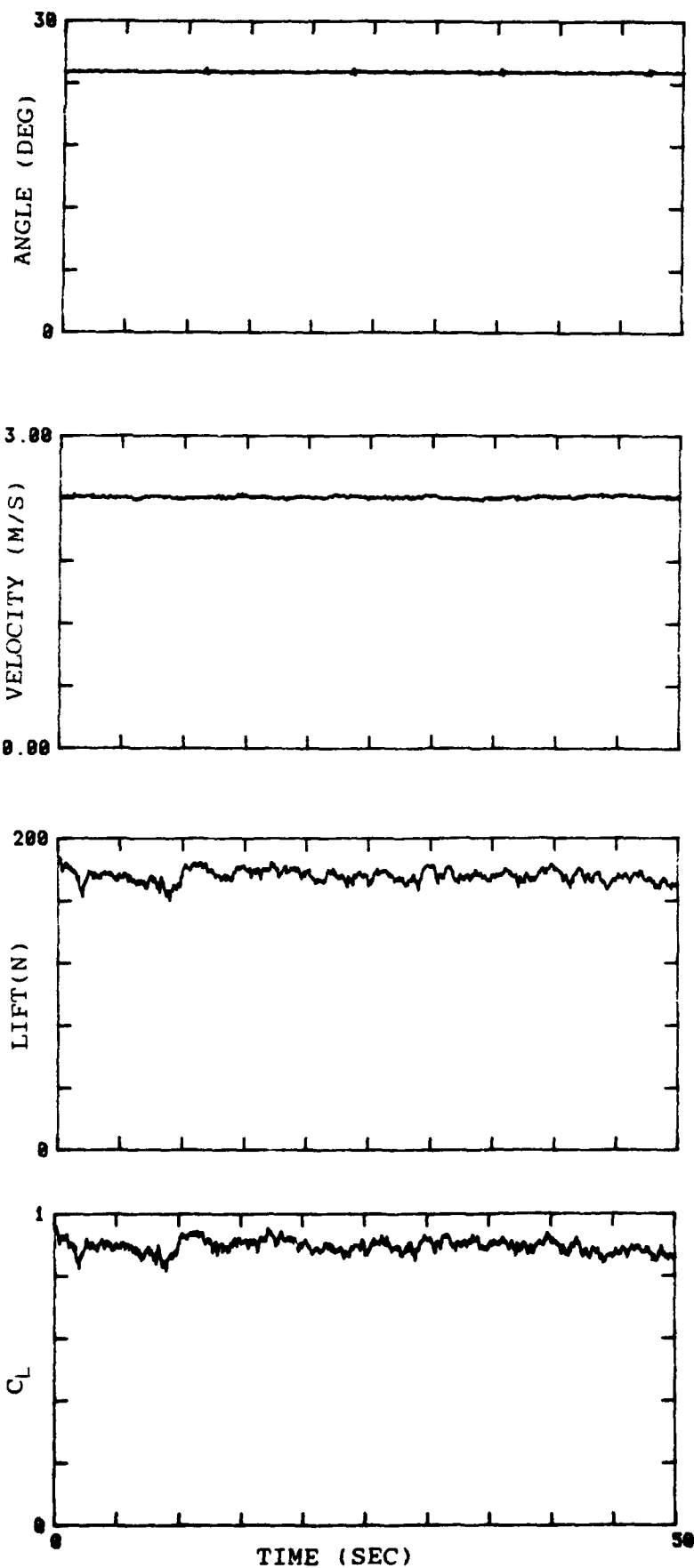


FIG.6 STATIC TIME HISTORY

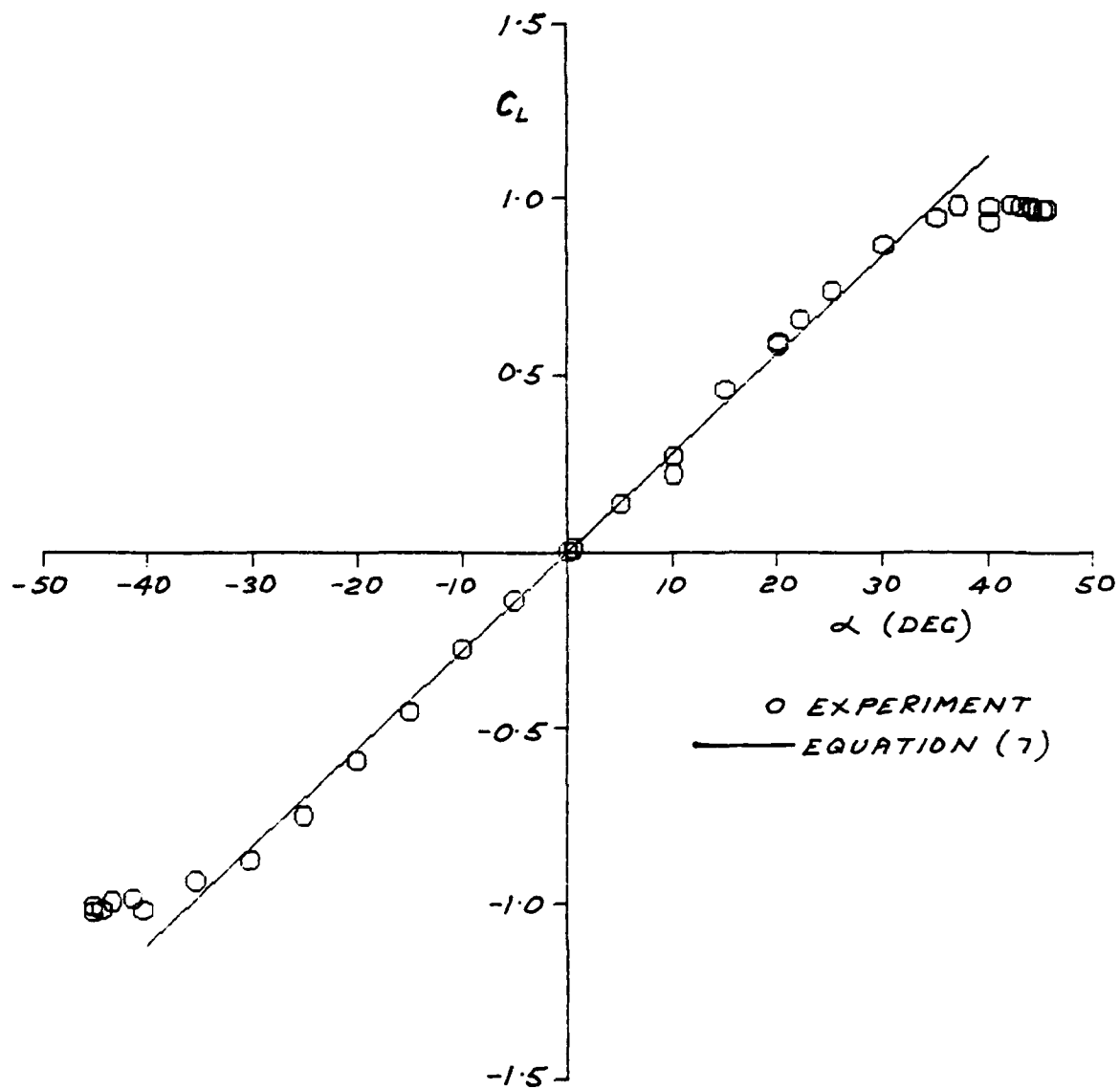


FIG. 7. LIFT COEFFICIENT- ASPECT RATIO 1, STATIC
CONDITION

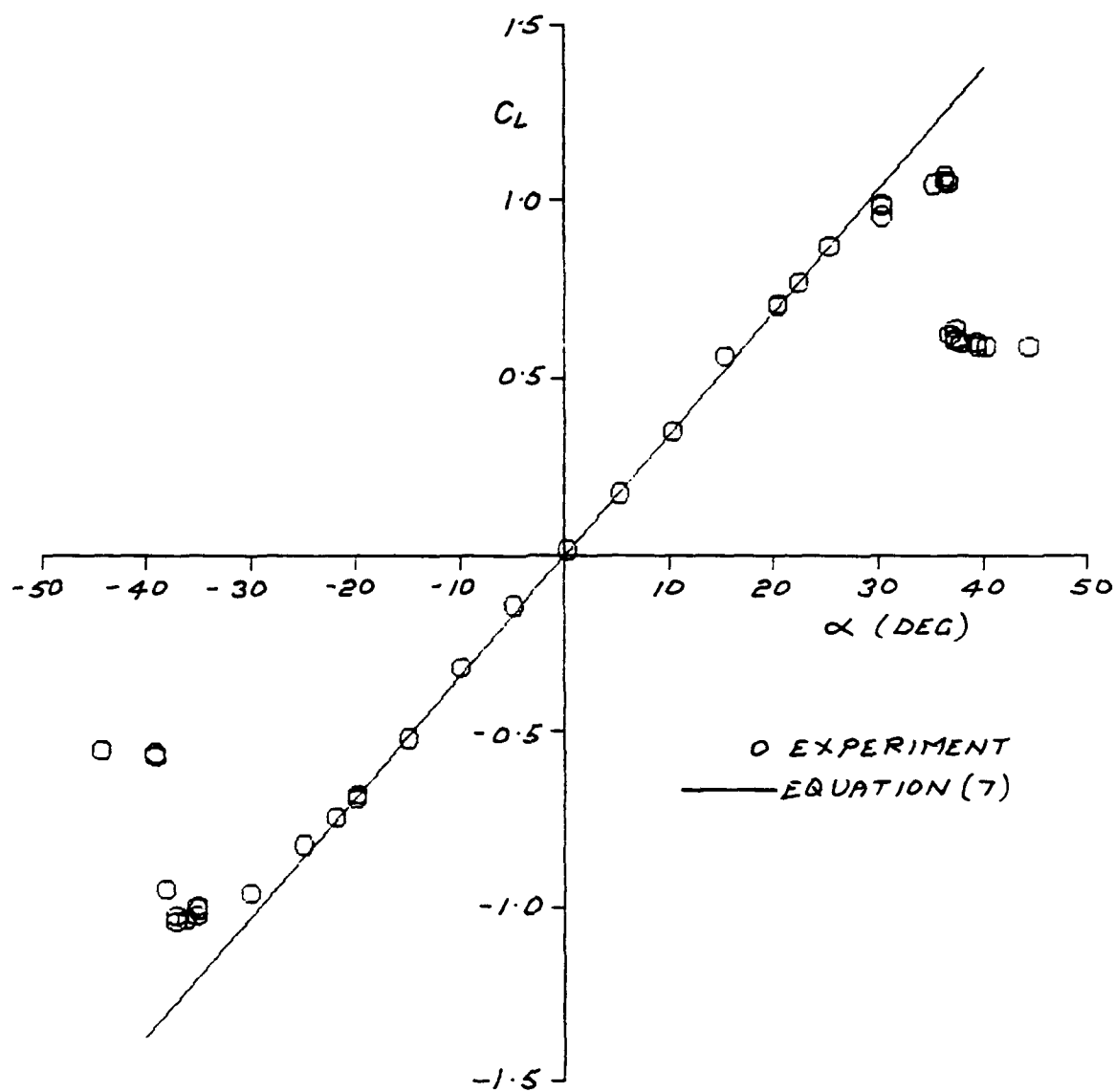


FIG. 8. LIFT COEFFICIENT—ASPECT RATIO 1.5, STATIC CONDITION

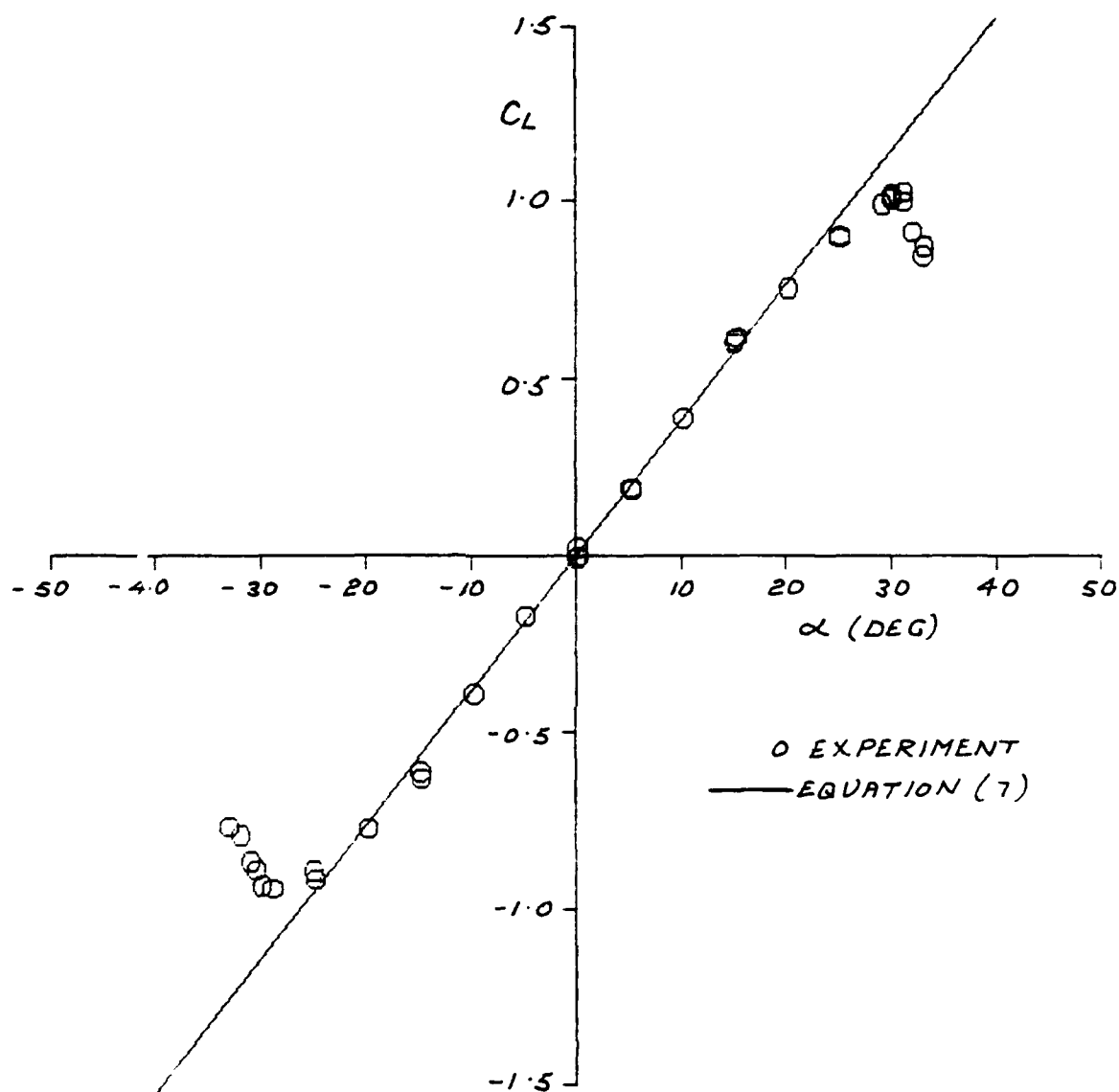


FIG. 9. LIFT COEFFICIENT - ASPECT RATIO 2, STATIC CONDITION

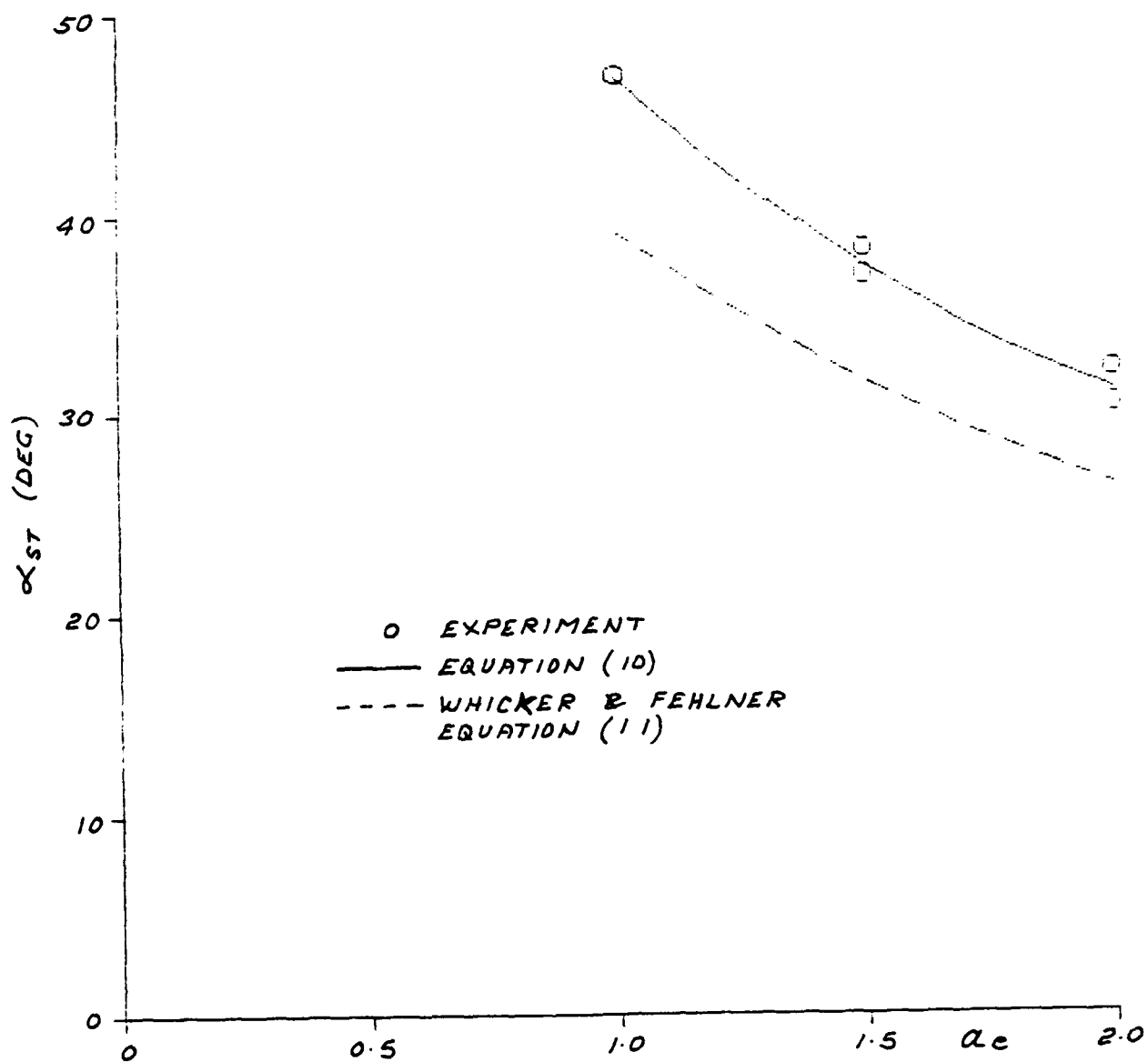


FIG. 10. STALL ANGLE - STATIC CONDITION

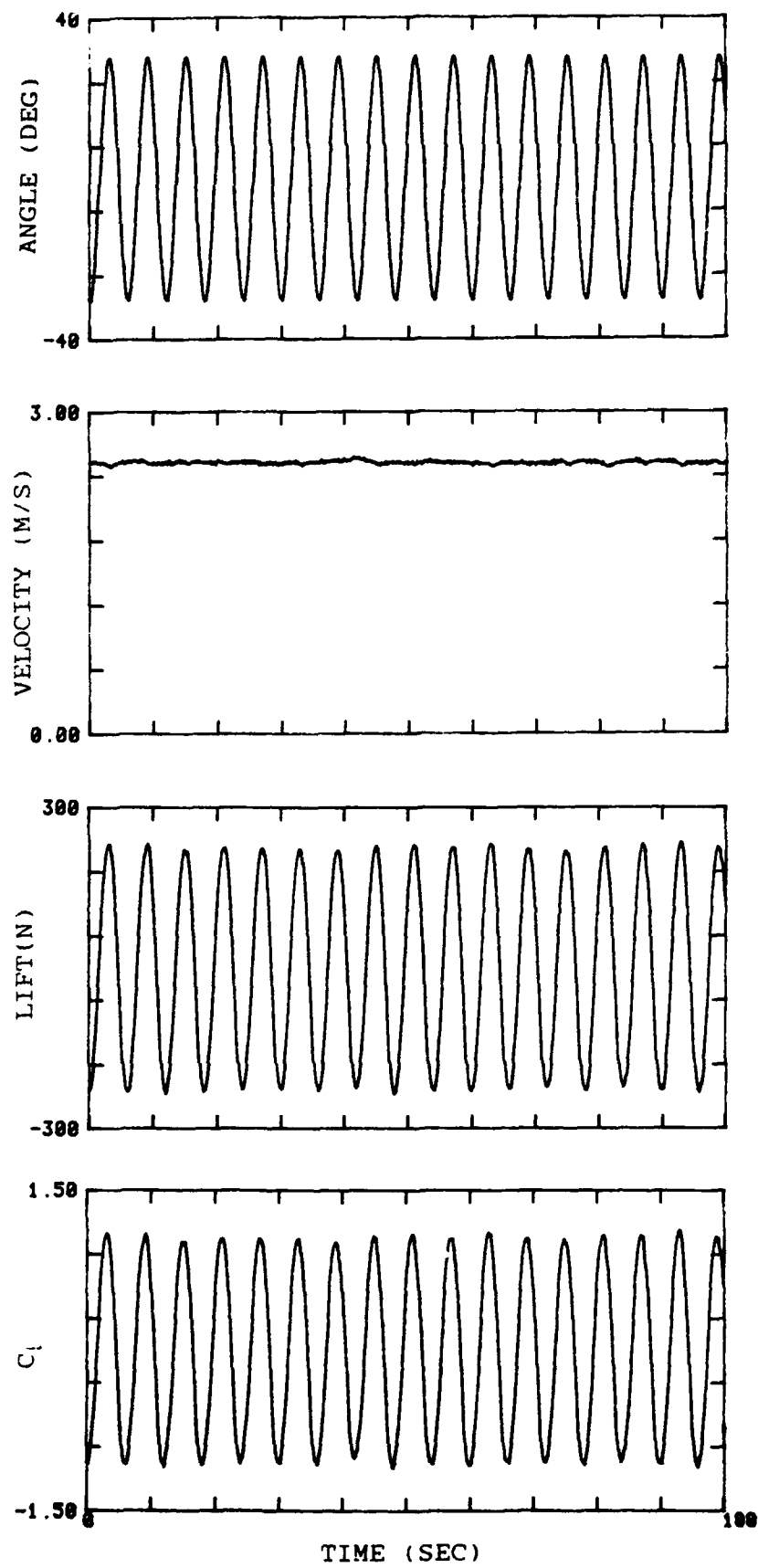


FIG.11 DYNAMIC TIME HISTORY

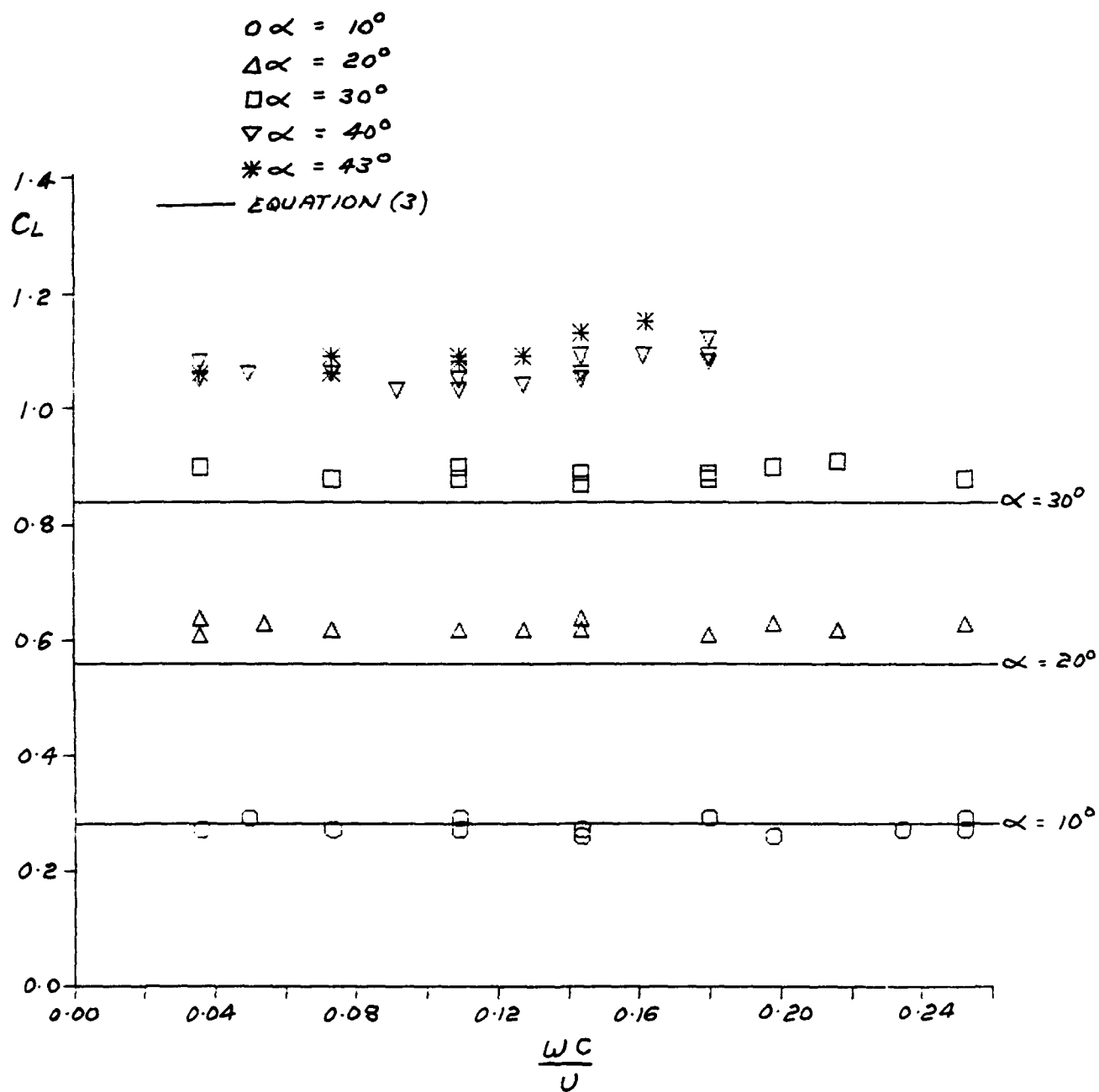


FIG. 12. LIFT COEFFICIENT ASPECT RATIO 1, DYNAMIC CONDITION

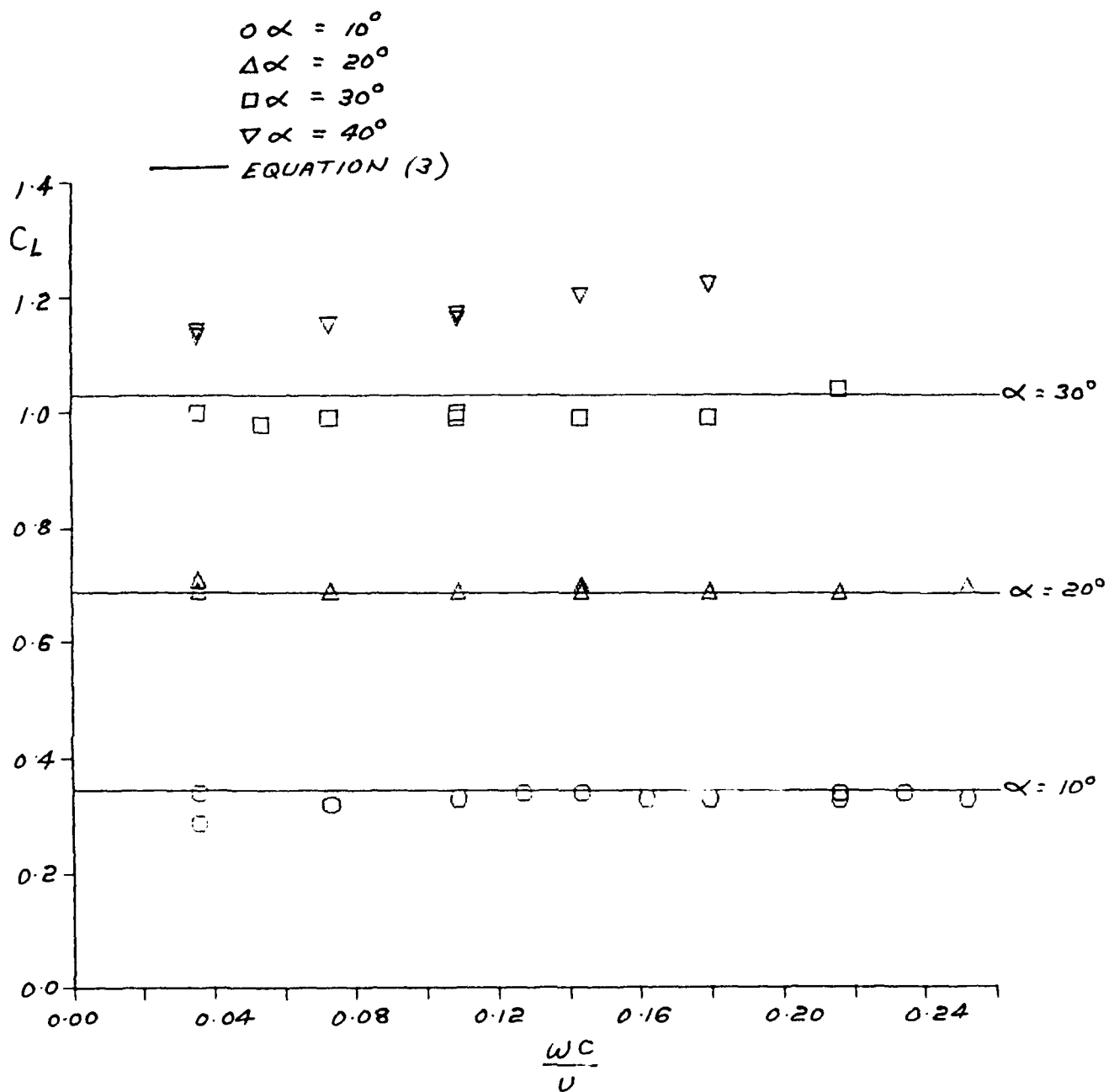


FIG. 13. LIFT COEFFICIENT - ASPECT RATIO 1.5, DYNAMIC CONDITION

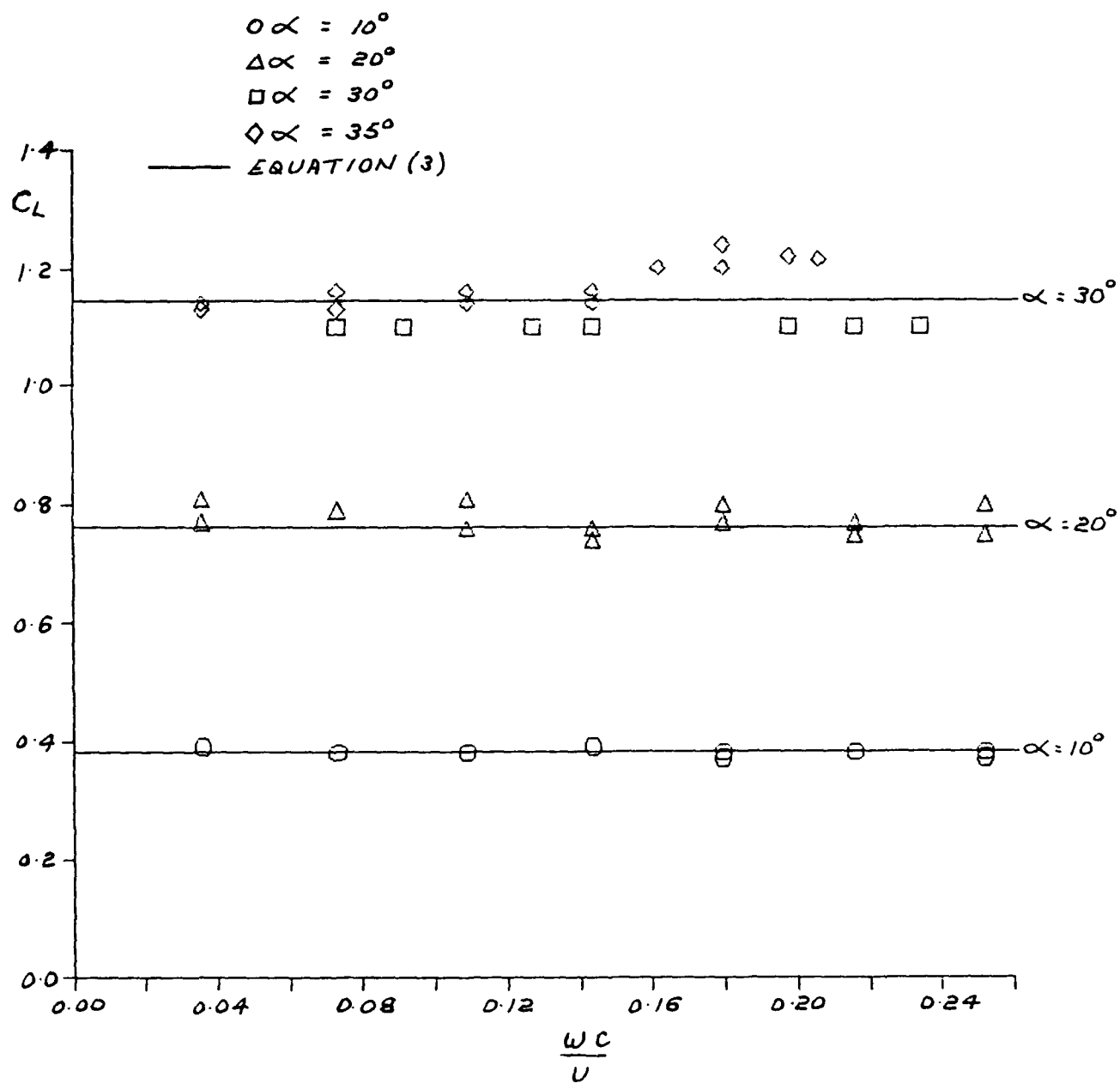


FIG. 14. LIFT COEFFICIENT-ASPECT RATIO 2, DYNAMIC CONDITION

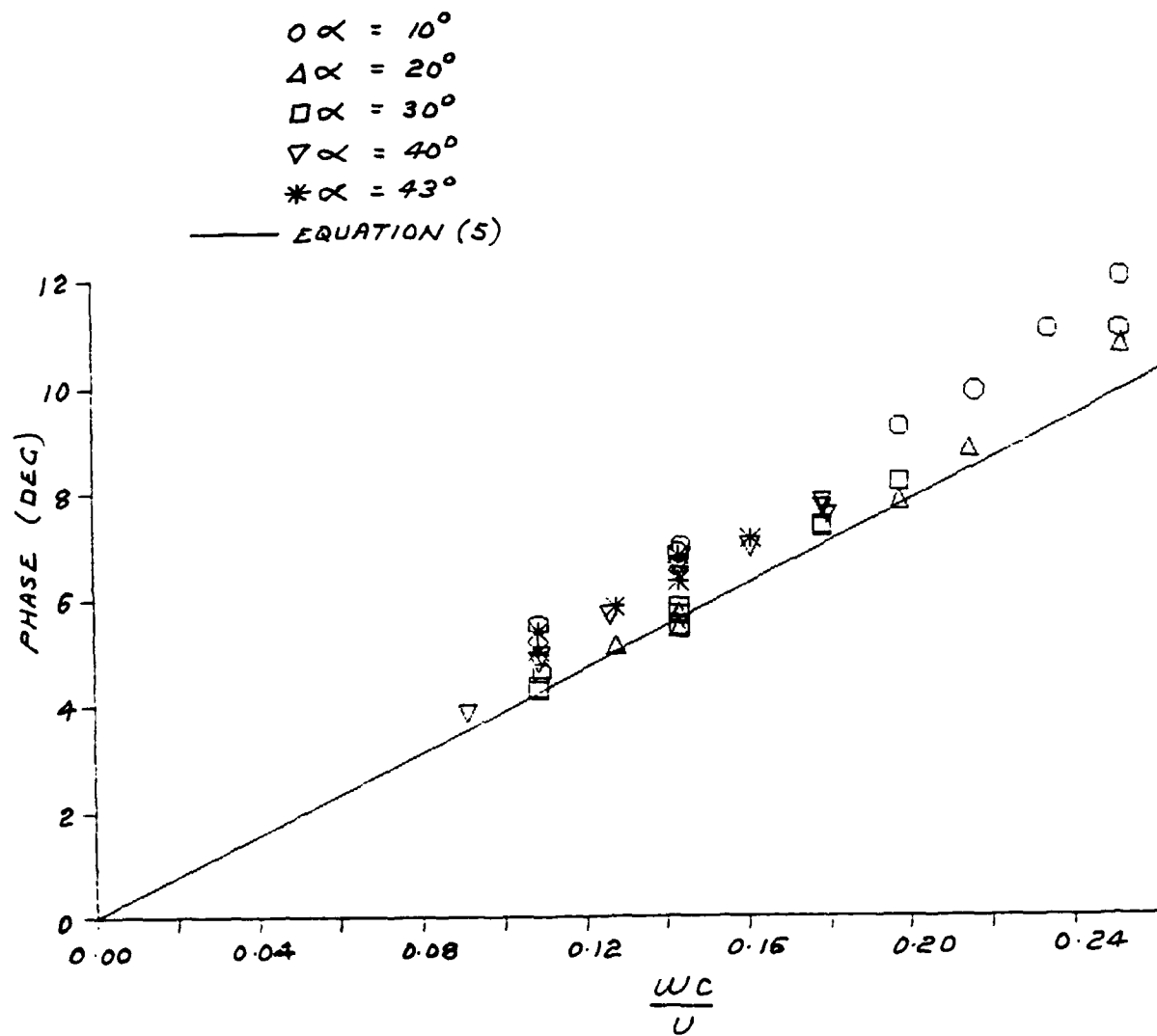


FIG. 15. PHASE ANGLE — ASPECT RATIO 1

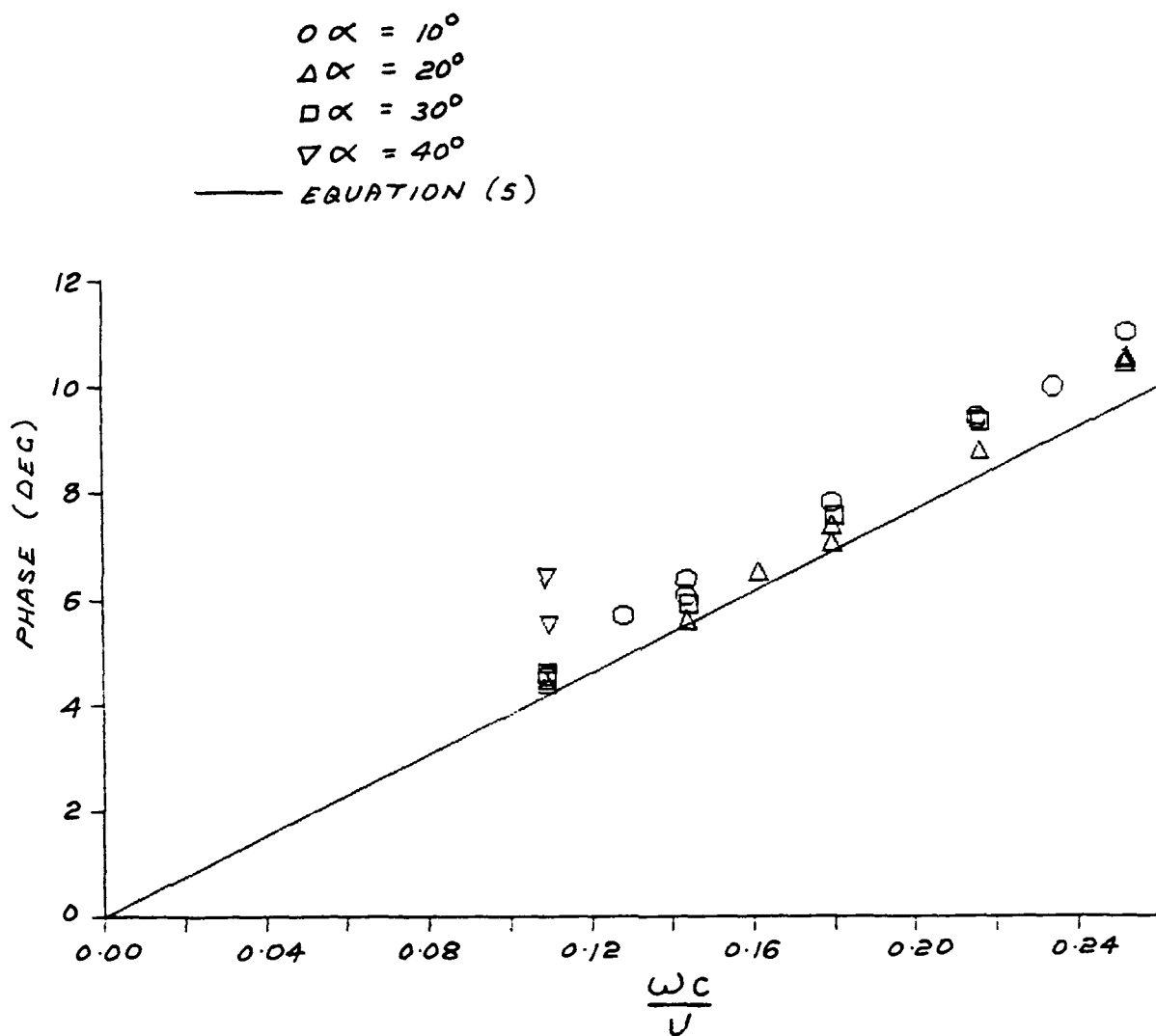


FIG. 16. PHASE ANGLE - ASPECT RATIO 1.5

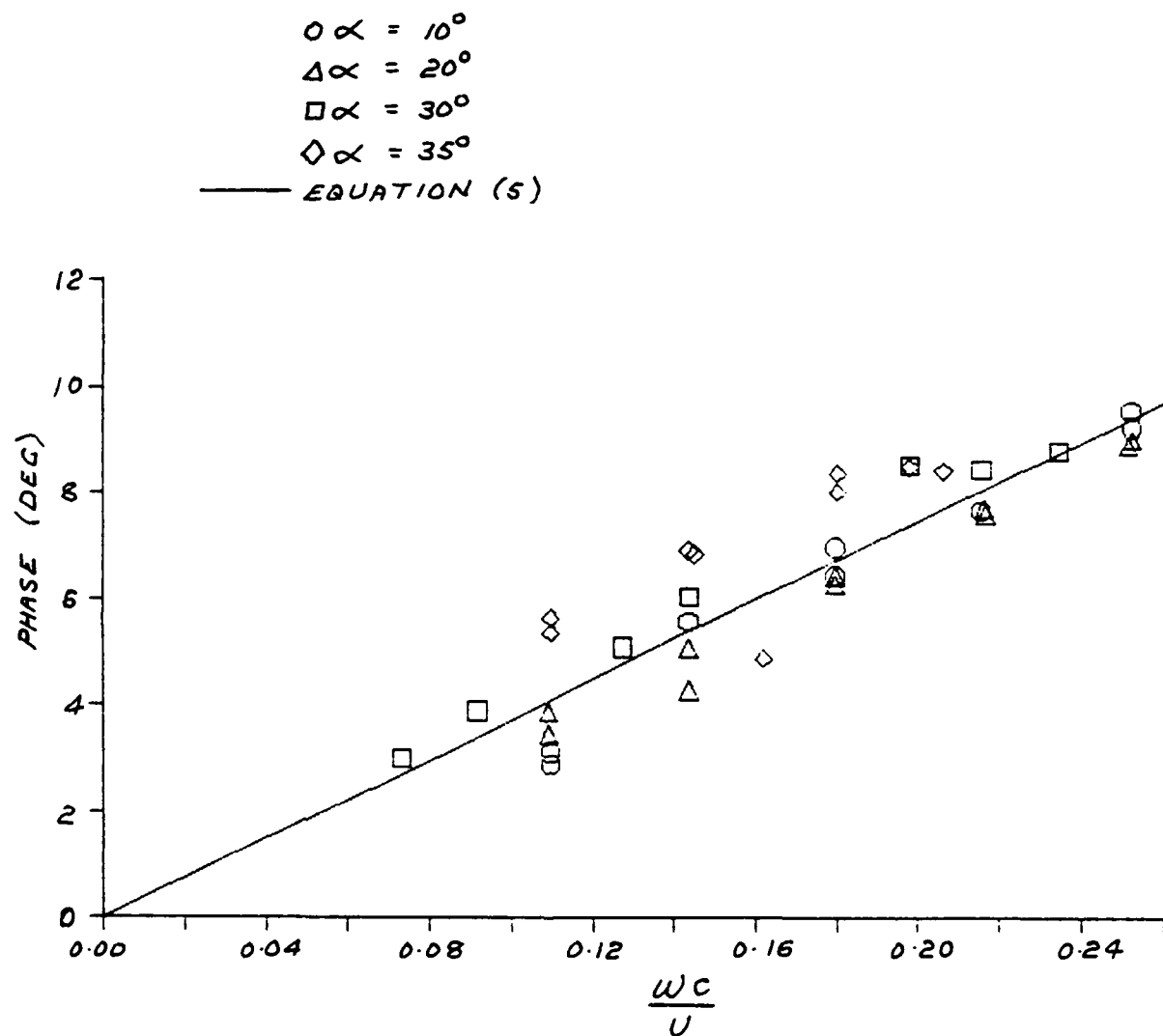


FIG. 17. PHASE ANGLE - ASPECT RATIO 2

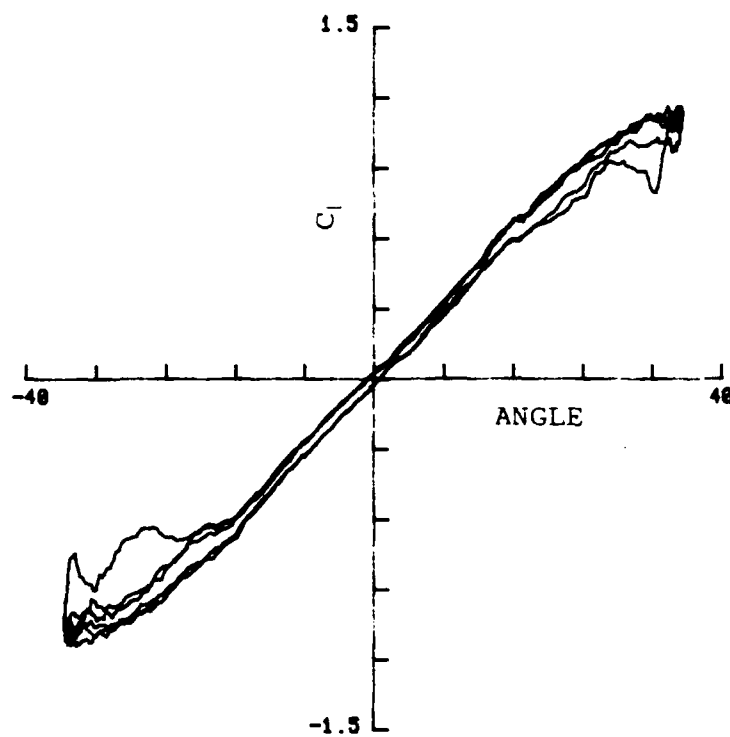


FIG.18(1) DYNAMIC CONDITION - ASPECT RATIO 2
35.5 DEGREES , FREQUENCY 0.055HZ

$$\frac{\omega c}{U} = 0.036$$

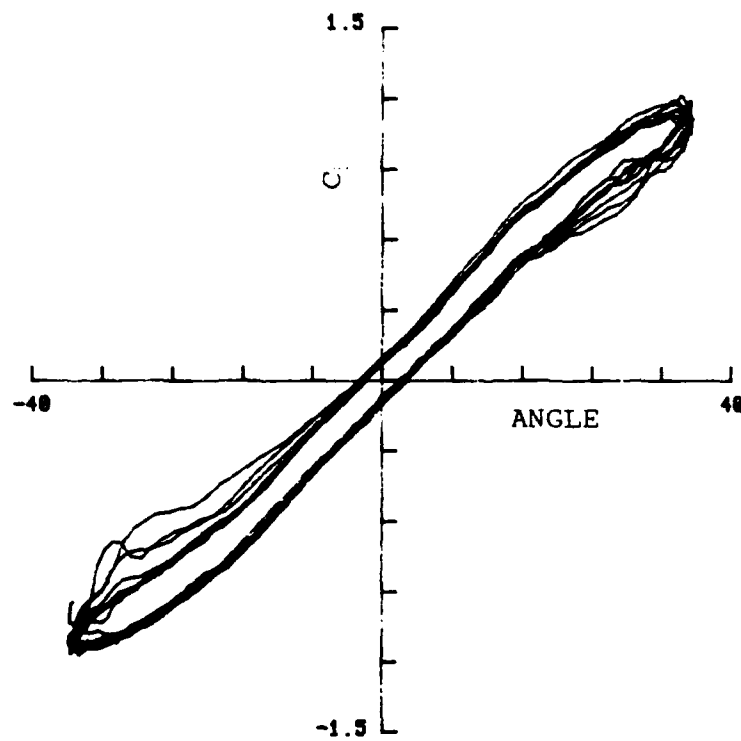


FIG.18(11) DYNAMIC CONDITION - ASPECT RATIO 2
35.5 DEGREES , FREQUENCY 0.168HZ

$$\frac{\omega C}{U} = 0.11$$

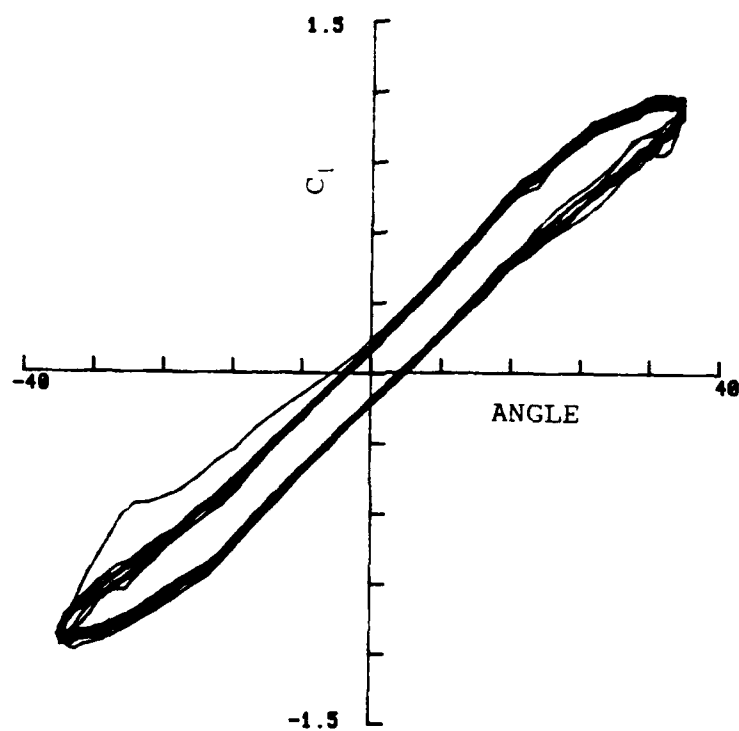


FIG.18(iii) DYNAMIC CONDITION - ASPECT RATIO 2
35.5 DEGREES , FREQUENCY 0.222HZ

$$\frac{\omega C}{U} = 0.145$$

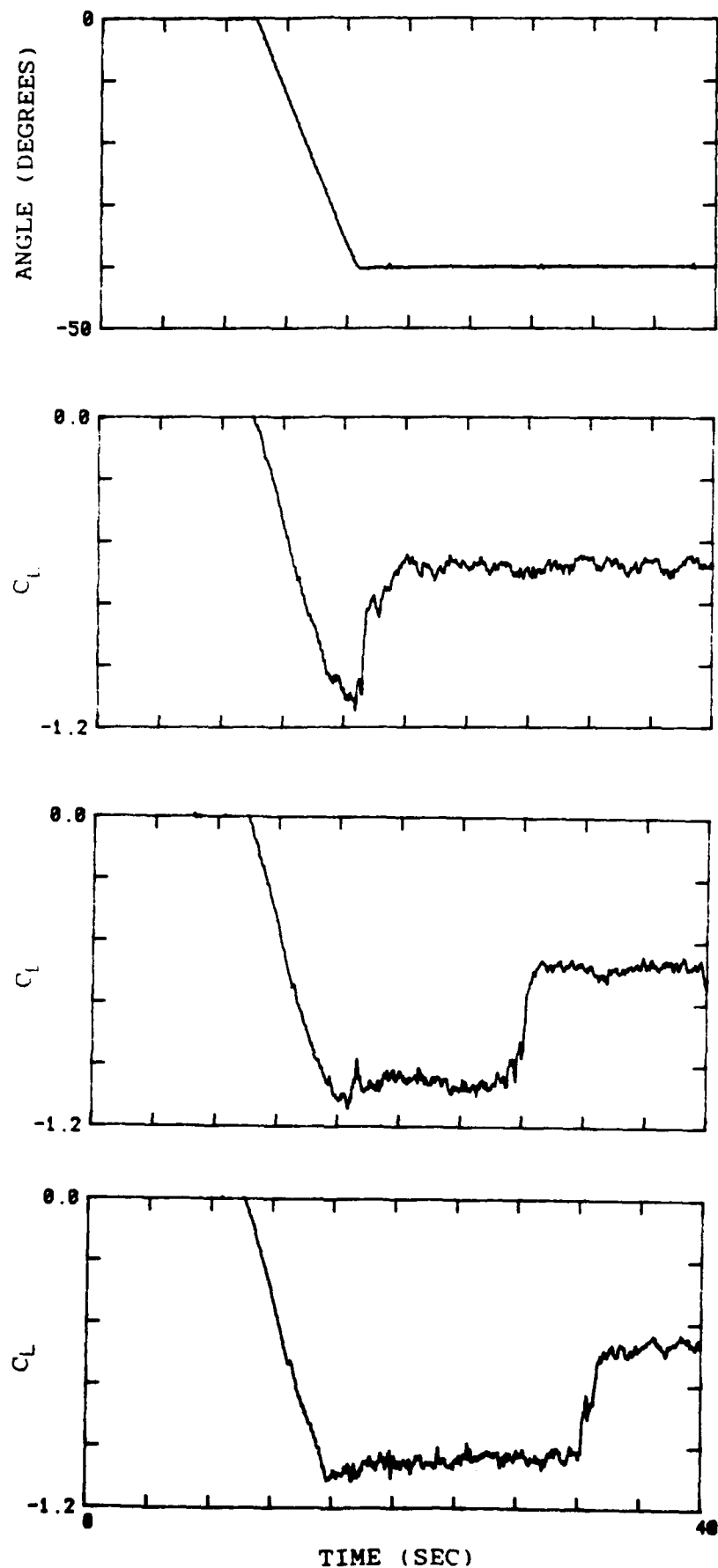


FIG.19 EXAMPLE OF DELAYED STALL - ASPECT RATIO 1.5
41 DEGREES, ANGULAR RATE 6 DEGREES/SEC

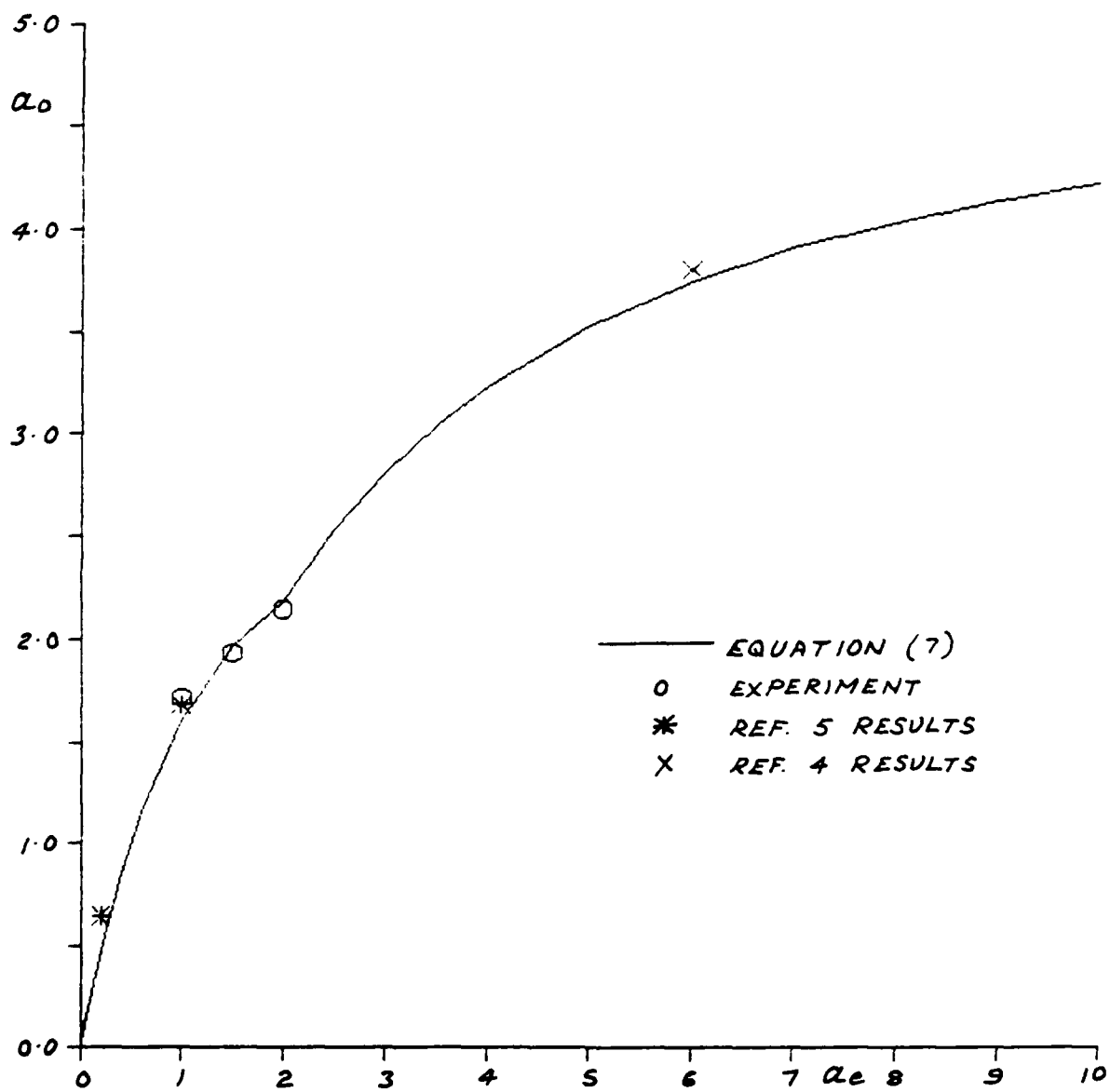


FIG. 20. EMPIRICAL FORMULA FOR COEFFICIENT Q_0

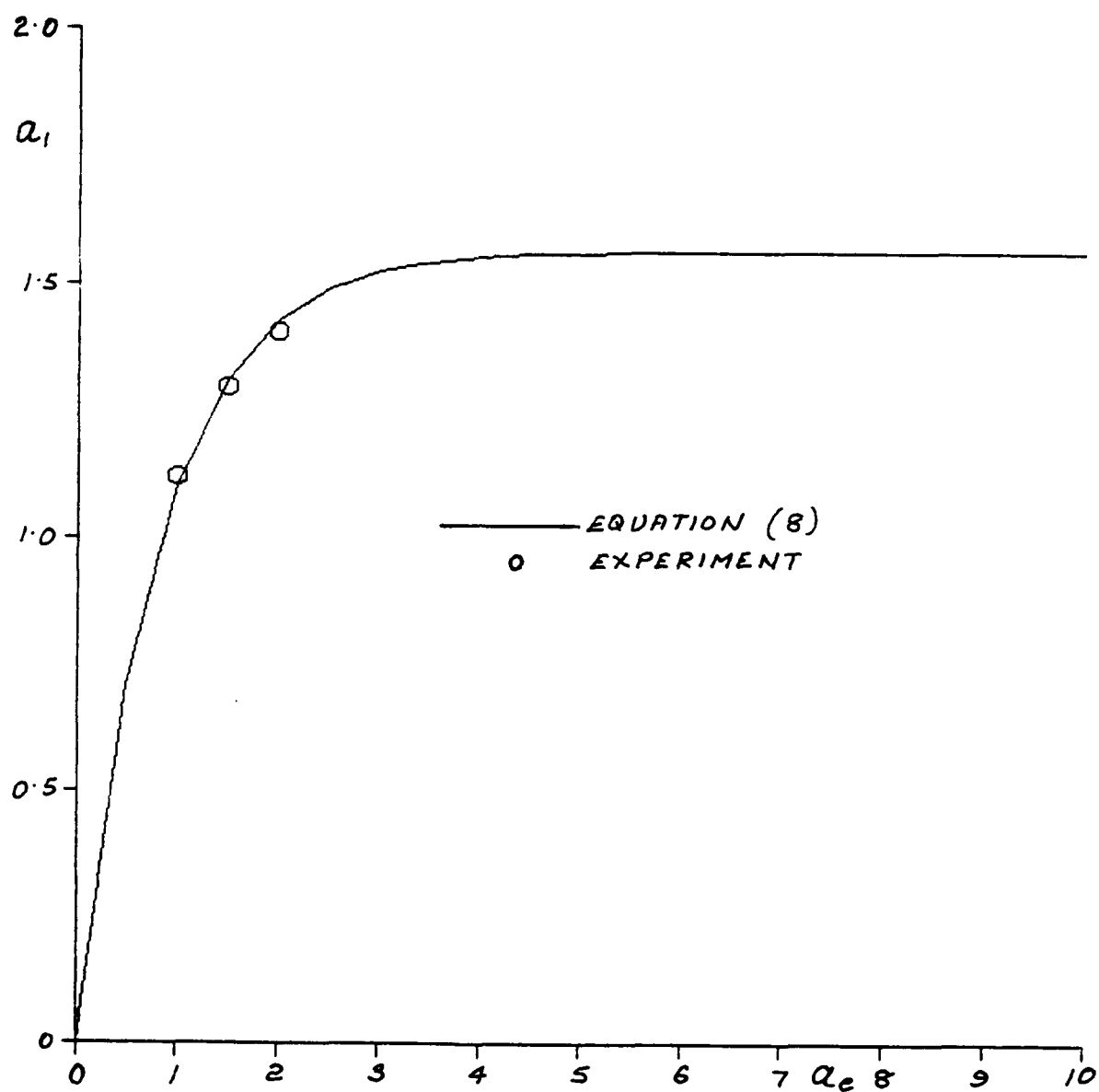


FIG. 21. EMPIRICAL FORMULA FOR COEFFICIENT Q_1

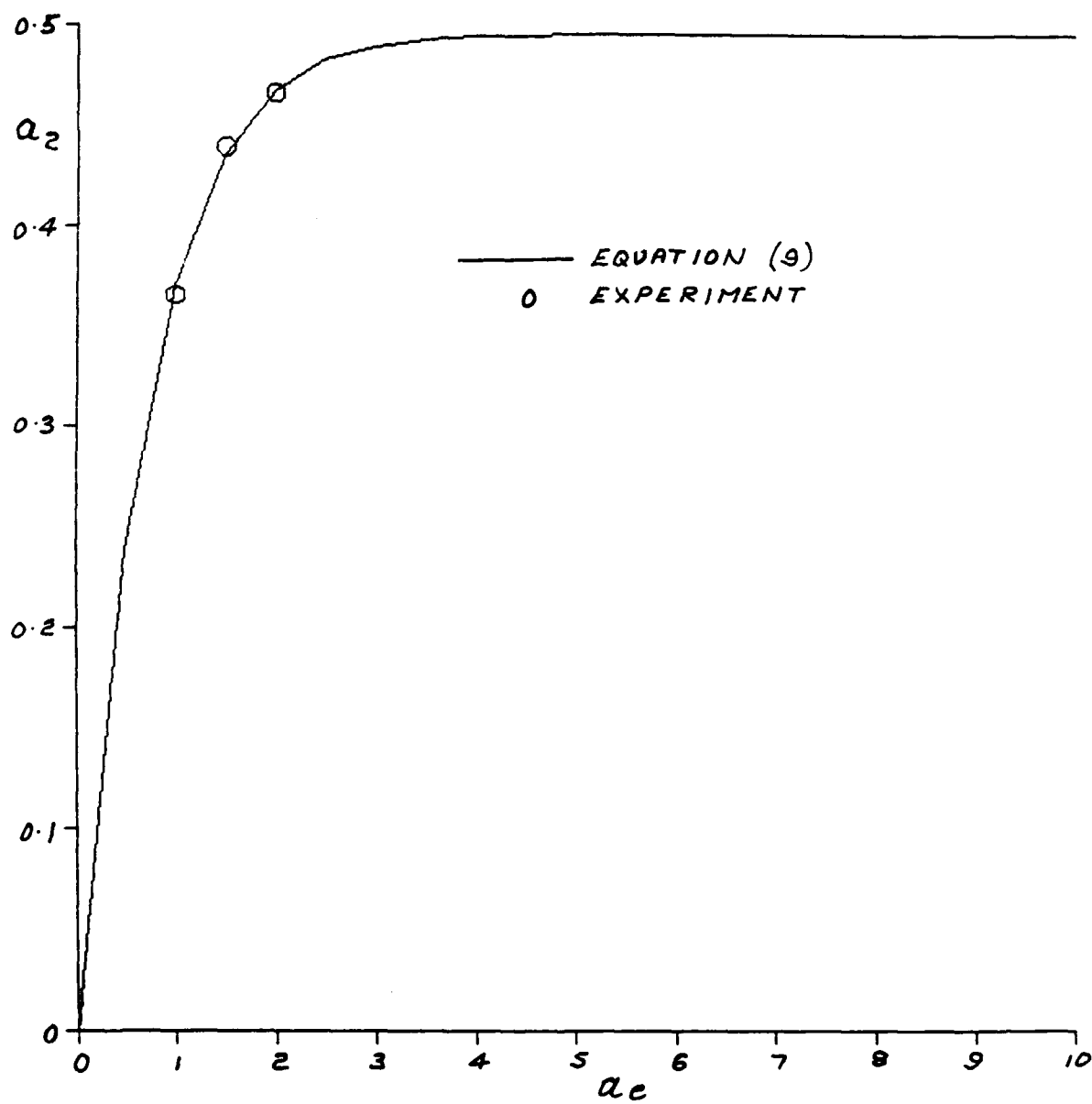


FIG. 22. EMPIRICAL FORMULA FOR COEFFICIENT Q_2

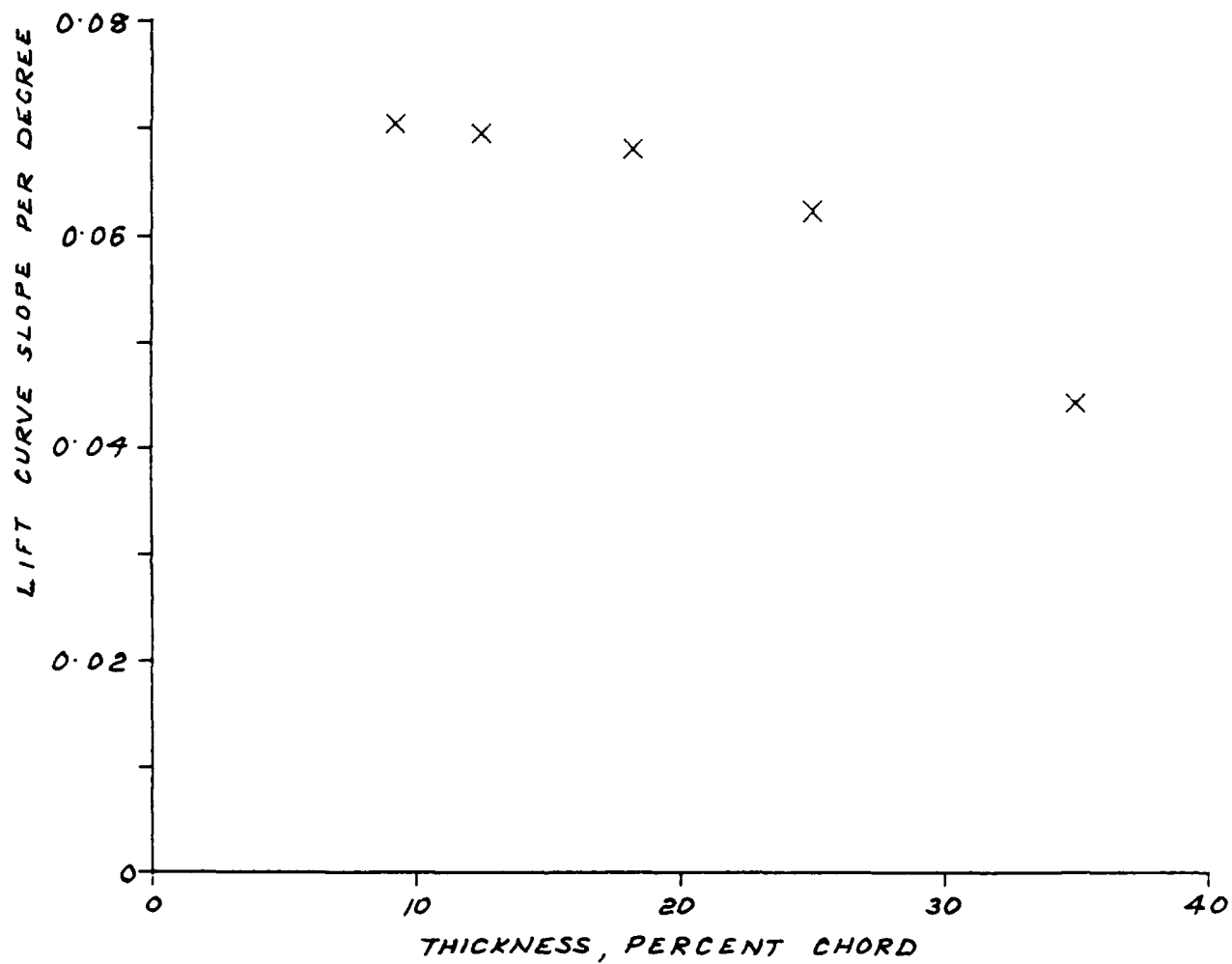


FIG. 23. EFFECT OF THICKNESS ON LIFT CURVE SLOPE
NACA OOX SERIES ASPECT RATIO 6 (REF 4)
 $R_e = 4 \times 10^6$

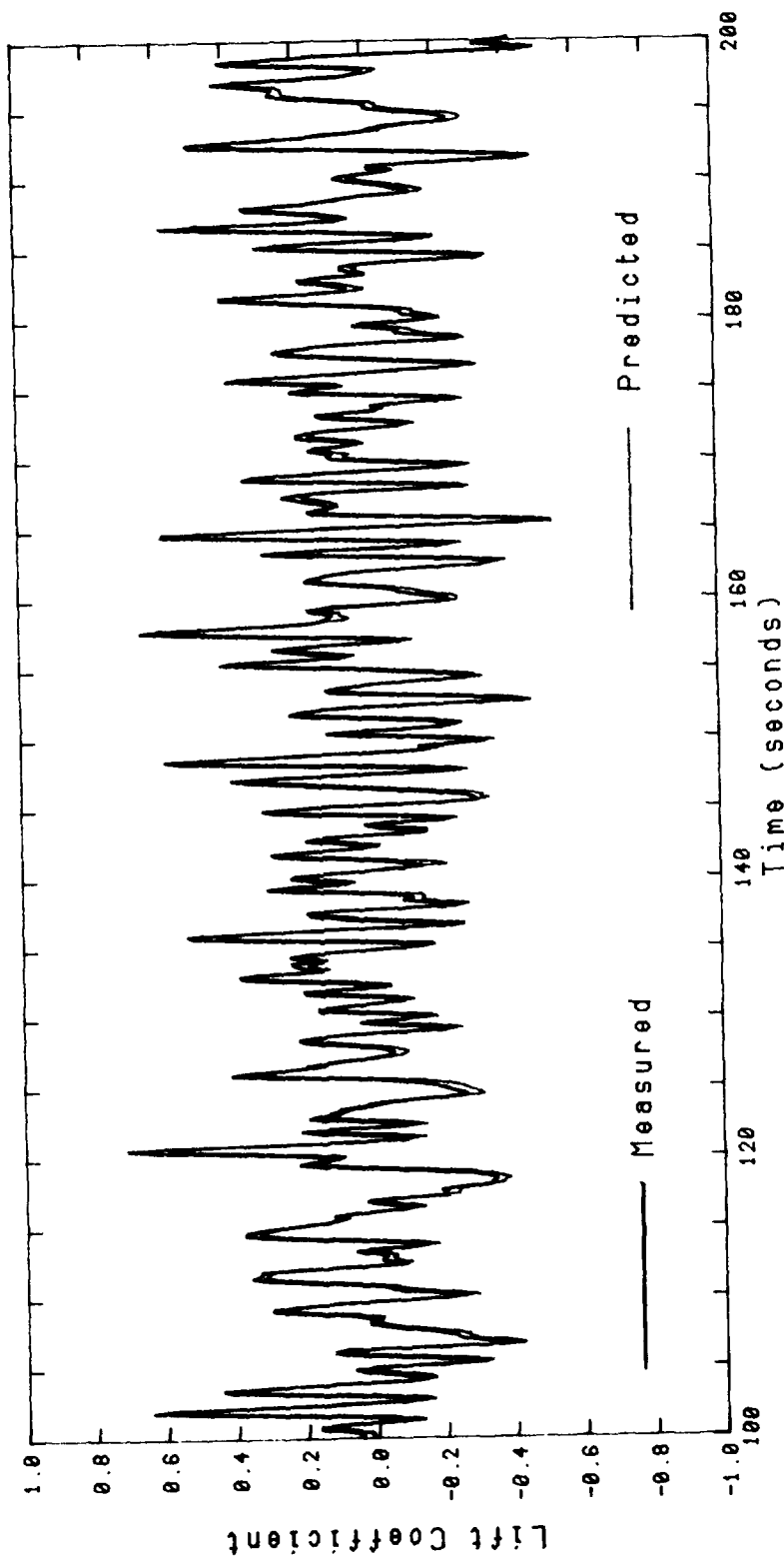


Fig 24 COMPARISON OF C_L FROM EQUATION (3)
WITH RANDOM SIGNAL RESULTS

REPORT DOCUMENTATION PAGE

DRIC Reference number (if known)

Overall security classification of sheet UNCLASSIFIED

(As far as possible this sheet should contain only unclassified information. If it is necessary to enter classified information, the field concerned must be marked to indicate the classification, eg (R), (C) or (S).

Originator's Reference/Report No ARE TM(UHR)90306		Month March	Year 1990
Originator's Name and Location Admiralty Research Establishment Haslar GOSPORT Hants PO12 2AG			
Monitoring Agency Name and Location			
Title EXPERIMENTS ON LOW ASPECT RATIO HYDROPLANES TO MEASURE LIFT UNDER STATIC AND DYNAMIC CONDITIONS			
Report Security Classification UK UNCLASSIFIED		Title Classification (U, R, C or S)	
Foreign Language Title (In the case of translations)			
Conference Details			
Agency Reference		Contract Number and Period	
Project Number		Other References	
Authors B WARD A R J M LLOYD			Pagination and Ref 9
Abstract This Technical Memorandum describes experiments in the Circulating Water Channel to measure lift forces on low aspect ratio hydroplanes under static and dynamic conditions. Empirical equations to represent the results are given.			
			Abstract Classification (U, R, C or S)
Descriptors			
Distribution Statement (Enter any limitations on the distribution of the document)			